JACS
JOURNAL OF THE AMERICAN CHEMICAL SOCIETY
Communication
pubs.acs.org/JACS

High-Efficiency Polymer Solar Cells via the Incorporation of an Amino-Functionalized Conjugated Metallopolymer as a Cathode Interlayer

Shengjian Liu, Kai Zhang, Junming Lu, Jie Zhang, Hin-Lap Yip, Fei Huang,* and Yong Cao

Institute of Polymer Optoelectronic Materials and Devices, State Key Laboratory of Luminescent Materials and Devices, South China University of Technology, Guangzhou 510640, P. R. China

Supporting Information

ABSTRACT: An amino-functionalized conjugated metallopolymer PFEN-Hg was developed as a cathode interlayer for inverted polymer solar cells. The resulting devices exhibited significantly improved performance with power conversion efficiencies exceeding 9%. Moreover, good device performance was achievable with the PFEN-Hg over a wider range of film thickness, likely due to the Hg−Hg interactions and improved $\pi-\pi$ stacking.

Polymer-fullerene bulk heterojunction solar cells (PSCs) have attracted much attention due to their potential application in flexible, lightweight, and large-area devices through low-cost solution processing.[1] Considering the practical aspects for commercialization, the inverted PSCs (I-PSCs), consisting of a photoactive layer between the ITO bottom cathode and the air-stable high-work-function (W_F) metal (typically, Al, Ag, Au, *etc.*) top anode, offer an advantageous approach given their superior long-term stability.[2] Moreover, the bulk-heterojunction (BHJ) films in I-PSCs undergo the desired vertical phase separation with a composition gradient that favors charge transport and collection, which can significantly improve photovoltaic device performance.[3]

The I-PSCs fabricated with a bare ITO cathode exhibit inferior performance because the high W_F of the ITO cathode (~4.8 eV) hinders the ohmic contact with the lowest unoccupied molecular orbital (LUMO) of the fullerene, reducing the open-circuit voltage (V_{oc}).[4] To achieve high-performance I-PSCs, an efficient strategy for reducing the W_F of the ITO and improving the electron collection property is required.[4] This goal can be realized through the insertion of an interlayer between the ITO and the photoactive layer. Several classes of materials have proven effective in improving the electron extraction properties of I-PSCs, including metal salts such as Cs_2CO_3,[5] CsF,[6] titanium chelate (TIPD, TOPD),[7] *etc.* The incorporation of an n-type metal oxide semiconductor such as ZnO,[8] TiO_x,[9] MoO_3−Al composite,[10] *etc.* can also improve the electron selectivity of the I-PSCs.

Alternatively, water-/alcohol-soluble polymeric/molecular interface materials have attracted great attention for I-PSCs, largely due to their solution processability and effective ITO modification properties.[11] The general design for these polymeric/molecular interface materials requires the introduction of specific functional groups (such as ethylene oxide,[12] phosphonate,[13] amino or ammonium,[14] *etc.*) that can form the desired interfacial dipole with the ITO substrate, thus reducing the W_F of ITO and significantly improving the charge-collection efficiency leading to high performance I-PSCs.[12−14]

Despite the advantages of easy solution processing and good film formation in the polymeric interface materials, these materials have the disadvantage of low conductivities, which render the solar cell performance strongly dependent on the thickness of the interlayer. Efficient devices can only be achieved with thin interlayer films.[12−14] Unfortunately, producing thin polymer films with good uniformity through the roll-to-roll coating process employed in the manufacture of large-area PSCs has proven challenging.[15] Therefore, interface materials that allow for a wider range of thicknesses are required. Moreover, tuning the optical spacer effect in the PSCs to maximize the light-harvesting property of the photoactive layer becomes more feasible with these materials.[16] Thus, the electrical conductivity of the polymeric interface materials must be further improved before they can be considered suitable components for the commercialization of PSCs.

Here, we aim to improve the I-PSC performance by introducing a rationally designed polymeric interlayer based on a conjugated metallopolymer with improved charge transport. Metal-based polymers/molecules have attracted much attention due to their intriguing spectroscopic, luminescence, and electrical properties,[17] and their propensity for exhibiting metal−metal (M−M) interactions that can provide additional means for manipulating the structural order and electronic coupling in organometallic compounds.[18] By tuning the molecular structures and the M−M interactions and by introducing new functionalities into the metallopolymers, several groups have successfully constructed highly ordered organometallic nanostructures with high electron and hole mobilities.[18] The new metallopolymer cathode interlayer examined in this work on I-PSCs is a Hg-containing derivative of amino-functionalized conjugated polymers (AFCPs), PFEN-Hg (see Scheme 1 for the chemical structure). Mercury was introduced due to its strong intermolecular, noncovalent Hg−Hg interactions,[19] which can increase the packing of the PFEN-Hg thin film. The PFEN-Hg is designed with several important properties required by an efficient interlayer: First, the PFEN-Hg possesses orthogonal solvent processability and good film

Received: August 21, 2013
Published: October 2, 2013

   dx.doi.org/10.1021/ja408363c | J. Am. Chem. Soc. 2013, 135, 15326−15329

Scheme 1. (a) Synthetic Route for the PFEN-Hg, and the Chemical Structures of PFN-OX, PFEO-Hg, PFEN, PTB7, and $PC_{71}BM$; (b) I-PSC Device Configuration

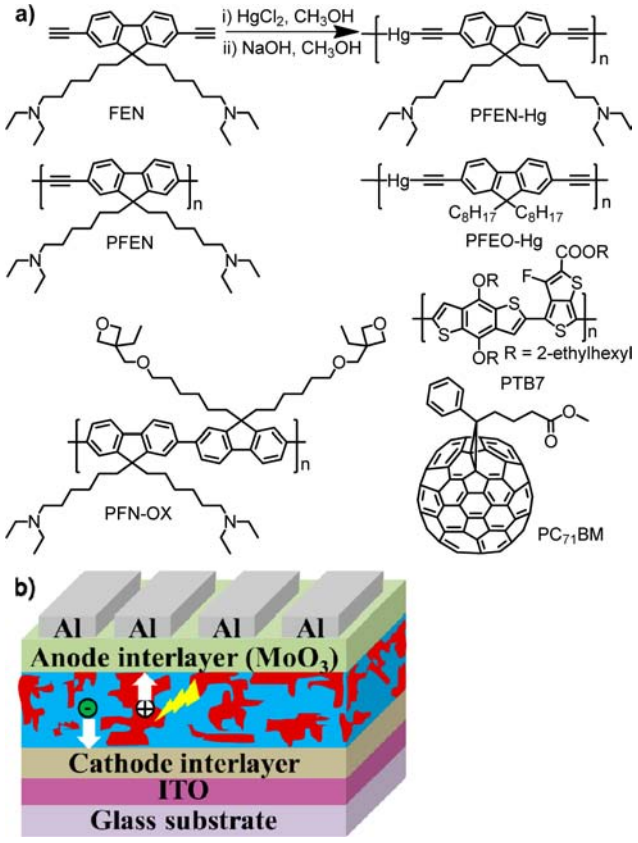

formation, which are critical for constructing multilayer devices via all-solution processes. The PFEN-Hg has excellent solubility in tetrahydrofuran (THF) and 1,4-dioxane, but is almost insoluble in chlorobenzene (CB) and dichlorobenzene (*o*-DCB), which are typically used to process the upper photoactive layer, thus making it a suitable interface material for the I-PSC applications. Second, PFEN-Hg can effectively reduce the W_F of the ITO because the amino-functionalized side chains facilitate the formation of the desired dipole with the ITO substrate, allowing it to efficiently extract electrons.[20] Third, the large band gap in the PFEN-Hg can better confine the excitons in the active layer and minimize the quenching of the excitons at the cathode interface.[21] Fourth, PFEN-Hg does not absorb light in the visible and near-infrared (NIR) regions, which minimizes the optical loss via interlayer absorption and therefore provides optimal light harvesting conditions for the active layer. Moreover, the introduction of the M−M interactions promotes stronger stacking of the polymer, which improves charge transport.[18] With these desired properties, the I-PSCs incorporated with a PFEN-Hg interlayer exhibited a substantially improved power conversion efficiency (PCE)—from 3.18% for an unmodified device to 9.11% under optimized conditions with a blend of [6,6]-phenyl C_{71}-butyric acid methyl ester ($PC_{71}BM$) and poly[4,8-bis(2-ethylhexyloxyl)benzo[1,2-*b*:4,5-*b*′]dithiophene-2,6-diyl-*alt*-ethylhexyl-3-uorothithieno[3,4-*b*]thiophene-2-carboxylate-4,6-diyl] (PTB7)[22] as the photoactive layer (see Scheme 1 for the chemical structures and device configuration). In addition, the device performance was relatively insensitive to the thickness of the PFEN-Hg. The I-PSC with a PFEN-Hg interlayer of ∼20 nm maintained a high PCE up to 8.6%, while the PCEs of the devices based on a nonmetalated reference polymer interlayer were nonperforming at a similar thickness. Our results indicated that PFEN-Hg is a promising interlayer for I-PSCs and can potentially be used in printed devices that require improved processing windows.

The synthetic route for the PFEN-Hg is provided in Scheme 1. The amino groups were introduced on the side chains of the PFEN-Hg to reduce the W_F of the ITO and improve the charge extraction.[20] For comparison, PFEO-Hg[23] and PFEN with structures similar to that of PFEN-Hg were synthesized. A cross-linkable PFN-OX[20] interlayer material specially designed for the I-PSCs was also used as a reference. The detailed synthesis procedures as well as solvent resistance and morphology studies of the PFEN-Hg and cross-linked PFN-OX are provided in the Supporting Information (SI).

The absorption spectra of the PFEN-Hg and PFEN polymers and the FEN monomer in THF and as thin-films are provided in Figure 1a. In comparison with the FEN monomer, the

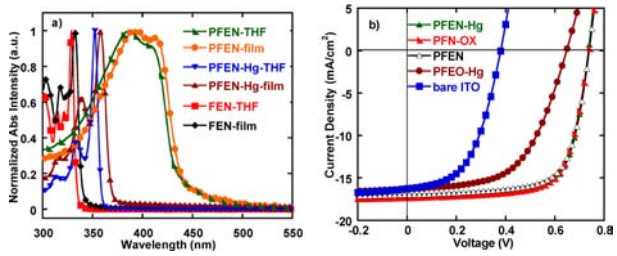

Figure 1. (a) Normalized absorption spectra of FEN, PFEN-Hg, and PFEN in both THF solutions and films. (b) *J*−*V* characteristics of the I-PSCs without an interlayer and with PFEO-Hg, PFEN, PFN-OX, and PFEN-Hg interlayers.

absorption spectra of the PFEN-Hg polymer were red-shifted by ∼30 nm both in solution and as a thin film due to the extended d−π conjugation after the inclusion of a heavy metal atom in the polymer backbone.[23] In contrast, the absorption spectra of the PFEN-Hg was significantly blue-shifted when compared to that of the PFEN, causing decreased optical absorption at visible wavelengths, which maximizes the number of photons reaching the photoactive layer. The PFEN-Hg exhibited a bathochromic shift of approximately 10 nm for the lowest-energy absorption band in the film when compared with the solution data. This phenomenon may be caused by an increased polymer chain aggregation and mercuriophilic interactions in the solid state.[19,23] The optical band gaps in the PFEN, PFEN-Hg, and FEN films were 2.81, 3.35, and 3.65 eV, respectively. The absorption data, the highest occupied molecular orbital (HOMO) energies, and the LUMO energies for the FEN, PFEN-Hg, and PFEN are summarized in Table S1 (see SI).

To investigate the interfacial modification effect of the PFEN-Hg on the I-PSCs, a PTB7:$PC_{71}BM$ blend was used as the photoactive layer with an ITO/interlayer/PTB7:$PC_{71}BM$/MoO_3/Al device configuration. A series of PFEN-Hg films of varying thicknesses were spin-coated atop an ITO from its 1,4-dioxane solution to create an interlayer. For comparison, devices were fabricated with different interlayers including PFEN, PFEO-Hg,[23] and a cross-linked PFN-OX.[20] A control device without any interlayer was also fabricated.

The current density−voltage (*J*−*V*) curves for the I-PSCs measured under AM 1.5G irradiation (100 mW cm^{-2}) are

dx.doi.org/10.1021/ja408363c | J. Am. Chem. Soc. 2013, 135, 15326−15329

presented in Figure 1b, and the corresponding EQE spectra are provided in Figure S6 (see SI). The J_{sc}, V_{oc}, FF, and PCE values are summarized in Tables 1 and S3 (see SI). The I-PSC with a

Table 1. Photovoltaic Properties of the I-PSCs with Various Interlayers under AM 1.5G Irradiation (100 mW cm^{-2})

interlayer	V_{oc} [V]	J_{sc} [mA cm^{-2}]	FF [%]	PCE [%]	R_s[a] [Ω cm^2]
bare ITO	0.38	16.29	51.3	3.18	6.4
PFEO-Hg	0.65	16.37	56.2	5.98	9.9
PFEN	0.74	16.97	70.0	8.80	4.2
PFN-OX	0.74	17.35	70.3	9.03	5.0
PFEN-Hg	0.74	17.37	71.2	9.11	4.4

[a]Series resistance (R_s) is deduced from the J–V curves.

bare ITO electrode exhibited a PCE of 3.18%, with a J_{sc} of 16.29 mA cm^{-2}, a V_{oc} of 0.38 V, and an FF of 51.3%. After a thin layer of cross-linked PFN-OX with an optimized thickness of 4 nm was inserted, the PCE reached 9.03%. A device with a 13-nm thin PFEN-Hg cathode interlayer exhibited an even higher PCE of 9.11% with an enhanced FF of 71.2%, a V_{oc} of 0.74 V, and a J_{sc} of 17.37 mA cm^{-2}, which is among the highest single-junction PSCs. The V_{oc}, J_{sc}, and FF of the ITO/PFEN-Hg device were simultaneously enhanced relative to the bare ITO electrode device, which led to significantly improved device performance. The control device using a thin PFEN interlayer with pendent amino groups also exhibited good device performance (a PCE of 8.80%, a J_{sc} of 16.97 mA cm^{-2}, an FF of 70.0%, and a V_{oc} of 0.74 V), while the ITO/PFEO-Hg device exhibited a moderate PCE of 5.98% with significantly decreased FF (56.2%) and V_{oc} (0.65 V) values due to the ineffectiveness of the W_F modification of the ITO substrate in the absence of amino-functionalized side chains. The W_F's of the bare ITO and the interlayer-modified ITOs were measured from the secondary electron cutoff of the X-ray photoelectron spectra (see SI, Figure S7).[24] The W_F of the ITO decreased from 4.8 to 4.5 eV when modified with PFEO-Hg and was further reduced to 4.0–4.2 eV when the amino-functionalized interlayers were applied. These data are consistent with the observed V_{oc} values in different I-PSCs. A maximum V_{oc} was obtained for the PFEN-, PFN-OX-, and PFEN-Hg-modified devices when the W_F of the cathode matched the LUMO energy of the $PC_{71}BM$ (~4.2 eV). In addition to the high V_{oc}'s, the respective FFs of ~70% in all devices with amino-functionalized interlayers also accounted for the high PCEs. We attribute the high FFs to the improved charge selectivity at the cathode interface, as indicated by the significantly reduced dark current under reversed bias in the J–V plot of the corresponding devices (see SI, Figure S8).[25] This result indicates that the amino-functionalized interlayers possess good hole-blocking properties and prevent hole current leakage through the cathode interface at reversed bias. In addition, the amino groups in the PFN side chain were recently found to be hole-trapping centers that can act as an effective hole-blocking layer[25c] and can optimize the rectification ratio and thus increase the FF of the devices. Moreover, the J_{sc} values of all I-PSC devices were well matched with those obtained via the integration of the corresponding EQE spectra (see SI, Figure S6, and Table S2).

The effect of the thickness of the PFN-OX and PFEN-Hg interlayers on the I-PSC performance was also examined, and the J–V characteristics are presented in Figure 2 with their corresponding J_{sc}, V_{oc}, FF, and PCE values summarized in Table 2. The performance of the PFN-OX-based devices was

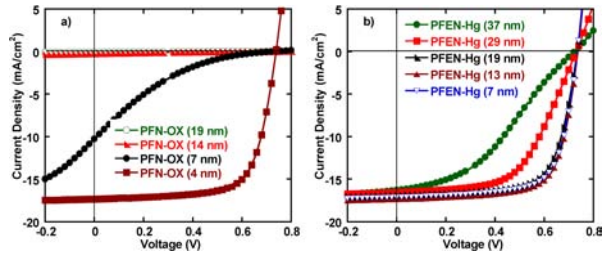

Figure 2. J–V characteristics of the I-PSCs with PFN-OX (a) and PFEN-Hg (b) interlayers of varying thickness under AM 1.5G irradiation (100 mW cm^{-2}).

Table 2. Photovoltaic Properties of the I-PSCs with PFN-OX and PFEN-Hg Interlayers of Varying Thickness under AM 1.5G Irradiation (100 mW cm^{-2})

interlayer (thickness)	V_{oc} [V]	J_{sc} [mA cm^{-2}]	FF [%]	PCE [%]	Rs[a] [Ω cm^2]
PFN-OX					
4 nm	0.74	17.35	70.3	9.03	5.9
7 nm	0.74	10.28	13.4	1.02	519
14 nm	0.74	0.25	0.17	0.03	8457
19 nm	0.74	0.08	0.18	0.01	19 029
PFEN-Hg					
7 nm	0.73	17.12	70.8	8.90	4.3
13 nm	0.74	17.37	71.2	9.11	4.4
19 nm	0.73	16.89	69.7	8.64	5.0
29 nm	0.73	16.55	56.5	6.82	13.9
37 nm	0.73	16.30	38.1	4.50	37.0

[a]Series resistance (Rs) is deduced from the J–V curves.

extremely sensitive to the cathode interlayer thickness. When the PFN-OX thickness increased slightly from the optimized thickness of 4–7 nm, the PCE dropped from 9% to 1% with poor diode characteristics as indicated by the shape of the J–V curve. The series resistance of the corresponding devices increased nearly 90-fold from 5.9 to 519 Ω cm^2 due to the poor charge transport property of PFN-OX. Further increases in interlayer thickness resulted in an insulator-like device with no photovoltaic response.

When PFEN-Hg was used as the interlayer, the optimized thickness was ~13 nm yielding a device with a PCE of 9.11%. The series resistance of the devices increased from 4.3 to 5.0 Ω cm^2 only when the PFEN-Hg thickness increased from 7 to 19 nm. The PCE remained above 8.6% even with a relatively thick (19 nm) PFEN-Hg film. Further increases in the thickness resulted in a gradual decrease in the device performance due to resistance loss in the interlayer. However, the PFEN-Hg-based device performance exhibited a less stringent dependency on the thickness of the interlayer due to the improved electron transport capabilities of the new interface material.

To investigate the electron transport properties of the interlayers, electron-only devices comprising the PFEN-Hg and PFN-OX interlayers were fabricated and tested with an ITO/Al/interlayer/PTB7:$PC_{71}BM$/Ba/Al device configuration. The J–V curves of the PFN-OX- and PFEN-Hg-based electron-only devices are provided in Figure 3a and b, respectively. The electron-current density decreased significantly with increasing PFN-OX film thickness, while the PFEN-Hg electron-only devices exhibited no apparent change in their J–V characteristics when the PFEN-Hg film thickness increased from 7 to 19

dx.doi.org/10.1021/ja408363c | J. Am. Chem. Soc. 2013, 135, 15326–15329

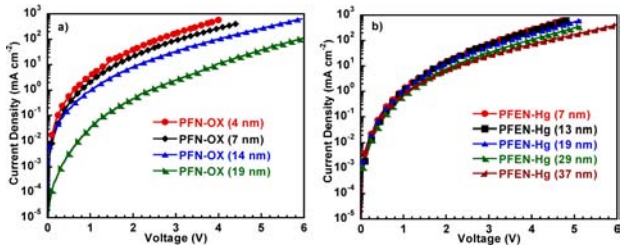

Figure 3. *J*–*V* curves of the electron-only devices with PFN-OX (a) and PFEN-Hg (b) interlayers of varying thickness. Electron-only device configuration: ITO/Al/interlayer/PTB7:$PC_{71}BM$/Ba/Al.

nm. This result further confirmed the improvement in the electron transport properties of the metallopolymer.

In conclusion, the metal-based conjugated polymer PFEN-Hg with pendent amino groups was synthesized and employed as an efficient interlayer for improving the electron transport and collection properties of high-performance I-PSCs. This new polymer offers the properties necessary for an efficient interface material including orthogonal solvent processability, good film formation, effective W_F modification of the ITO substrate, low optical absorption, good electron selectivity, and good electron transport properties. With these improved interfacial properties, the I-PSCs with PFEN-Hg interlayers exhibited encouraging PCE values of over 9%, which are among the best reported for single-junction PSCs. The new interface material offers an even more appealing feature in its ability to achieve good device performance with a wider range of film thicknesses, making large-area device processing possible. In addition, further work on pursuing environmentally friendly metallopolymers, which are more compatible with the roll-to-roll printing process, could allow for potential commercialization of organic photovoltaic technology.

■ ASSOCIATED CONTENT

Ⓢ Supporting Information

Experimental details regarding the synthesis, instruments, measurements, and fabrication procedures and characterization details of the I-PSC devices. This material is available free of charge via the Internet at http://pubs.acs.org.

■ AUTHOR INFORMATION

Corresponding Author

msfhuang@scut.edu.cn

Notes

The authors declare no competing financial interest.

■ ACKNOWLEDGMENTS

This work was financially supported by the Ministry of Science and Technology (No. 2014CB643501), the Natural Science Foundation of China (Nos. 21125419, 50990065, and 51010003), and the Guangdong Natural Science Foundation (No. S2012030006232).

■ REFERENCES

(1) (a) Beaujuge, P. M.; Fréchet, J. M. J. *J. Am. Chem. Soc.* **2011**, *133*, 20009. (b) Yu, G.; Gao, J.; Hummelen, J. C.; Wudl, F.; Heeger, A. J. *Science* **1995**, *270*, 1789. (c) Thompson, B. C.; Fréchet, J. M. J. *Angew. Chem., Int. Ed.* **2008**, *41*, 58. (d) Cheng, Y. J.; Yang, S. H.; Hsu, C. S. *Chem. Rev.* **2009**, *109*, 5868. (e) Inganäs, O.; Zhang, F. L.; Andersson, M. R. *Acc. Chem. Res.* **2009**, *42*, 1731. (f) Li, Y. *Acc. Chem. Res.* **2012**, *45*, 723. (g) Greenham, N. C. *Philos. Trans. R. Soc. London, Ser. A* **2013**, *371*, 20110414.

(2) (a) Chen, L.-M.; Hong, Z.; Li, G.; Yang, Y. *Adv. Mater.* **2009**, *21*, 1434. (b) Hau, S. K.; Yip, H.-L.; Jen, A. K. Y. *Polym. Rev.* **2010**, *50*, 474. (c) Gong, X. *Polymer* **2012**, *53*, 5437.

(3) (a) Campoy-Quiles, M.; Ferenczi, T.; Agostinelli, T.; Etchegoin, P. G.; Kim, Y.; Anthopoulos, T. D.; Stavrinou, P. N.; Bradley, D. D. C.; Nelson, J. *Nat. Mater.* **2008**, *7*, 158. (b) Xu, Z.; Chen, L.-M.; Yang, G.; Huang, C.-H.; Hou, J.; Wu, Y.; Li, G.; Hsu, C.-S.; Yang, Y. *Adv. Funct. Mater.* **2009**, *19*, 1227.

(4) (a) Yip, H.-L.; Jen, A. K. Y. *Energy Environ. Sci.* **2012**, *5*, 5994. (b) Chen, L. M.; Xu, Z.; Hong, Z. R.; Yang, Y. *J. Mater. Chem.* **2010**, *20*, 2575.

(5) Li, G.; Chu, C. W.; Shrotriya, V.; Huang, J.; Yang, Y. *Appl. Phys. Lett.* **2006**, *88*, 253503.

(6) Reinhard, M.; Hanisch, J.; Zhang, Z.; Ahlswede, E.; Colsmann, A.; Lemmer, U. *Appl. Phys. Lett.* **2011**, *98*, 053303.

(7) Tan, Z.; Zhang, W.; Zhang, Z.; Qian, D.; Huang, Y.; Hou, J.; Li, Y. *Adv. Mater.* **2012**, *24*, 1476.

(8) (a) Yang, T.; Cai, W.; Qin, D.; Wang, E.; Lan, L.; Gong, X.; Peng, J.; Cao, Y. *J. Phys. Chem. C* **2010**, *114*, 6849. (b) Sun, Y.; Seo, J. H.; Takacs, C. J.; Seifter, J.; Heeger, A. J. *Adv. Mater.* **2011**, *23*, 1679.

(9) Waldauf, C.; Morana, M.; Denk, P.; Schilinsky, P.; Coakley, K.; Choulis, S. A.; Brabec, C. J. *Appl. Phys. Lett.* **2006**, *89*, 233517.

(10) Liu, J.; Shao, S.; Fang, G.; Meng, B.; Xie, Z.; Wang, L. *Adv. Mater.* **2012**, *24*, 2774.

(11) (a) Huang, F.; Wu, H.; Cao, Y. *Chem. Soc. Rev.* **2010**, *39*, 2500. (b) Hoven, C. V.; Garcia, A.; Bazan, G. C.; Thuc-Quyen, N. *Adv. Mater.* **2008**, *20*, 3793. (c) Duan, C.; Zhang, K.; Zhong, C.; Huang, F.; Cao, Y. *Chem. Soc. Rev.* DOI: 10.1039/C3CS60200A.

(12) Zhou, Y.; Li, F.; Barrau, S.; Tian, W.; Inganäs, O.; Zhang, F. *Sol. Energy Mater. Sol. Cells* **2009**, *93*, 497.

(13) (a) Zhu, Y.; Xu, X.; Zhang, L.; Chen, J. W.; Cao, Y. *Sol. Energy Mater. Sol. Cells* **2012**, *97*, 83. (b) Duan, C.; Zhong, C. M.; Liu, C. C.; Huang, F.; Cao, Y. *Chem. Mater.* **2012**, *24*, 1682.

(14) (a) Zhou, Y.; et al. *Science* **2012**, *336*, 327. (b) He, Z.; Zhong, C.; Su, S.; Xu, M.; Wu, H.; Cao, Y. *Nat. Photonics* **2012**, *6*, 591. (c) Yang, T.; Wang, M.; Duan, C.; Hu, X.; Huang, L.; Peng, J.; Huang, F.; Gong, X. *Energy Environ. Sci* **2012**, *5*, 8208. (d) Zhang, K.; Guan, X.; Huang, F.; Cao, Y. *Acta Chim. Sin.* **2013**, *70*, 2489. (e) Liu, S.; Zhang, Z.; Chen, D.; Duan, C.; Lu, J.; Zhang, J.; Huang, F.; Su, S.; Chen, J.; Cao, Y. *Sci. China: Chem.* **2013**, *56*, 1119.

(15) Krebs, F. C. *Sol. Energy Mater. Sol. Cells* **2009**, *93*, 465.

(16) (a) Kim, J. Y.; Kim, S. H.; Lee, H. H.; Lee, K.; Ma, W.; Gong, X.; Heeger, A. J. *Adv. Mater.* **2006**, *18*, 572. (b) Park, S. H.; Roy, A.; Beaupré, S.; Cho, S.; Coates, N.; J. Moon, S.; Moses, D.; Leclerc, M.; Lee, K.; Heeger, A. J. *Nat. Photonics* **2009**, *3*, 297.

(17) Ho, C.-L.; Wong, W.-Y. *Coord. Chem. Rev.* **2011**, *255*, 2469.

(18) Yuen, M. Y.; Roy, V. A.; Lu, W.; Kui, S. C.; Tong, G. S.; So, M. H.; Chui, S. S.; Muccini, M.; Ning, J. Q.; Xu, S. J.; Che, C. M. *Angew. Chem., Int. Ed.* **2008**, *47*, 9895.

(19) Wong, W. Y.; Choi, K. H.; Lu, G. L.; Lin, Z. Y. *Organometallics* **2002**, *21*, 4475.

(20) (a) Zhong, C.; Liu, S.; Huang, F.; Wu, H.; Cao, Y. *Chem. Mater.* **2011**, *23*, 4870. (b) Liu, S.; Zhong, C.; Zhang, J.; Duan, C.; Wang, X.; Huang, F. *Sci. China: Chem.* **2011**, *54*, 1745.

(21) Halls, J. J. M.; Pichler, K.; Friend, R. H.; Moratti, S. C.; Holmes, A. B. *Appl. Phys. Lett.* **1996**, *68*, 3120.

(22) Liang, Y.; Xu, Z.; Xia, J.; Tsai, S.-T.; Wu, Y.; Li, G.; Ray, C.; Yu, L. *Adv. Mater.* **2010**, *22*, E135.

(23) Wong, W. Y.; Liu, L.; Shi, J. X. *Angew. Chem., Int. Ed.* **2003**, *42*, 4064.

(24) Cahen, D.; Kahn, A. *Adv. Mater.* **2003**, *15*, 271.

(25) (a) Luo, J.; Wu, H.; He, C.; Li, A.; Yang, W.; Cao, Y. *Appl. Phys. Lett.* **2009**, *95*, 043301. (b) Seo, J. H.; Gutacker, A.; Sun, Y.; Wu, H.; Huang, F.; Cao, Y.; Scherf, U.; Heeger, A. J.; Bazan, G. C. *J. Am. Chem. Soc.* **2011**, *133*, 8416. (c) Duan, C.; Cai, W.; Hsu, B. B. Y.; Zhong, C.; Zhang, K.; Liu, C.; Hu, Z.; Huang, F.; Bazan, G. C.; Heeger, A. J.; Cao, Y. *Energy Environ. Sci.* **2013**, *6*, 3022.